



Cite this: *Dalton Trans.*, 2015, 44, 13003

Received 10th June 2015,  
Accepted 24th June 2015

DOI: 10.1039/c5dt02204e

www.rsc.org/dalton

## Dual luminescence in solid CuI(piperazine): hypothesis of an emissive 1-D delocalized excited state†

L. Maini,<sup>\*a</sup> D. Braga,<sup>a</sup> P. P. Mazzeo,<sup>b</sup> L. Maschio,<sup>\*c</sup> M. Rérat,<sup>d</sup> I. Manet<sup>e</sup> and B. Ventura<sup>\*e</sup>

**Solid [CuI(piperazine)<sub>0.5</sub>]<sub>∞</sub>, characterized by a structure with an infinite double chain of CuI, presents an unexpected dual luminescence. The short copper–copper distances allow the existence of both cluster-centered and 1-D delocalized electronic transitions, as emerged from theoretical calculations. Beyond the more common cluster-centered emission a higher energy band, which differs in lifetime and in temperature dependence, is observed.**

One of the most prominent classes of luminescent coordination compounds is that of copper(i) halides, due to their promising features for application in the field of optoelectronics.<sup>1–5</sup> They are easily synthesized<sup>6,7</sup> and tunable in emission color,<sup>8–10</sup> with high emission quantum yields in the solid state.<sup>7,10,11</sup> Copper(i) halide compounds can be considered as a valid alternative to luminescent metal complexes of precious (*i.e.* Ir or Os) and rare earth metals, which are expensive and environmentally problematic.<sup>12</sup>

The luminescence properties of the copper halide clusters arise from a remarkable variety of emissive states, which have been extensively investigated in the last 30 years and can be summarized as follows: (a) a low-energy emission, attributed to a triplet cluster-centered (<sup>3</sup>CC) excited state, is observed in the case of metal center interactions<sup>13–19</sup> and is independent of the nature of the ligand engaged in the complex; (b) a high-energy emission, attributed to a triplet halide-to-ligand charge transfer (<sup>3</sup>XLCT) excited state, may show up in the presence of unsaturated ligands with accessible  $\pi$ -orbitals.<sup>20</sup> Moreover,

recent studies have shown that several copper compounds present a thermally activated delayed fluorescence (TADF): Cu(i) halide-bridged compounds with P^N ligands are characterized by (metal + halide)-to-ligand charge transfer ((M + X) LCT) excited states where the low singlet–triplet energy gap allows emission from both the singlet and the triplet excited states, depending on the temperature.<sup>21–23</sup>

The structure of [CuI(piperazine)<sub>0.5</sub>]<sub>∞</sub><sup>24</sup> is characterized by a one-dimensional copper iodide polymeric structure. The infinite double chain of CuI is described as castellated,<sup>25</sup> as shown in Fig. 1a, and the tetrahedral coordination of the copper(i) ions is fulfilled by the bridging piperazine to construct a 3D network (Fig. 1b and c). The inorganic chain is generated by the sequence of an inversion center and 2-fold axis symmetry elements, thus two different copper distances are present (2.771(1) Å and 2.729(1) Å). Although the presence of infinite double chain motifs has been observed in 20 struc-

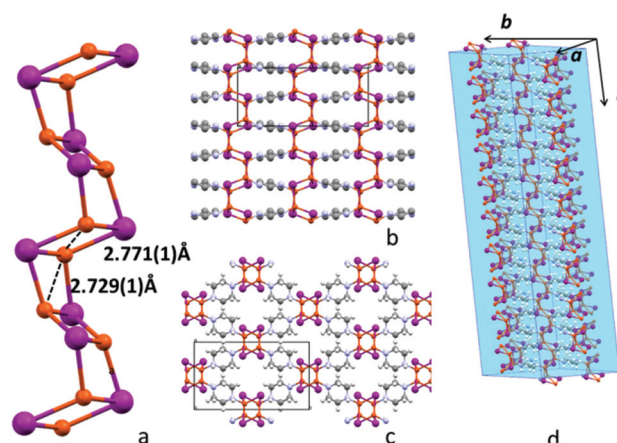


**Fig. 1** Crystal structure of [CuI(piperazine)<sub>0.5</sub>]<sub>∞</sub> (a) Infinite double chain of CuI (copper atoms are orange, iodide atoms are purple); (b) crystal packing view along the a-axis and c-axis pointing down; (c) crystal packing view along the c-axis; (d) scheme of the crystal morphology: crystals grow along the axis [001] which corresponds to the direction of the CuI chain.

<sup>a</sup>Dip. Chimica "G. Ciamician", Università di Bologna, Via Selmi 2, 40126 Bologna, Italy. E-mail: l.maini@unibo.it

<sup>b</sup>Excelsus Structural Solutions (Swiss) AG, c/o Paul Scherrer Institut WBB/011, 5232 Villigen PSI, Switzerland

<sup>c</sup>Dip. Chimica, Università di Torino, Via P. Giuria 5, 10125 Torino, Italy. E-mail: lorenzo.maschio@unito.it

<sup>d</sup>ECP IPREM UMR5254, Université de Pau et des Pays de l'Adour, 64000 Pau, France

<sup>e</sup>Istituto ISOF, Consiglio Nazionale delle Ricerche, Via P. Gobetti 101, 40129 Bologna, Italy. E-mail: barbara.ventura@isof.cnr.it

† Electronic supplementary information (ESI) available: Synthesis of the compound, data mining, spectroscopic data, computational methods. CCDC 1404771–1404773. For ESI and crystallographic data in CIF or other electronic format see DOI: 10.1039/c5dt02204e

tures present in the CSD,<sup>26</sup> only three other structures (CEZBEQ, AGIYEU01, and HUHJUP) in addition to  $[\text{CuI}(\text{piperazine})_{0.5}]_{\infty}$  have all metallic distances shorter than 2.80 Å, which is twice the van der Waals radius.<sup>27</sup> The other structures mainly show alternation of long (>2.80 Å) and short (<2.80 Å) distances between Cu–Cu atoms. In these cases the inorganic chain can be described as a sequence of dimers placed side by side while in the  $[\text{CuI}(\text{piperazine})_{0.5}]_{\infty}$  structure the CuI chain can be defined as an inorganic wire. Data collection on single crystal at low temperature shows the shortening of the Cu–Cu distances, which is in agreement with the red shift of the <sup>3</sup>CC emission band (see Table S2 in the ESI† and discussion below).

The luminescence properties of  $[\text{CuI}(\text{piperazine})_{0.5}]_{\infty}$  have been explored in the solid state both at room temperature and at 77 K. Solid  $[\text{CuI}(\text{piperazine})_{0.5}]_{\infty}$  shows an unexpected dual luminescence at room temperature: upon excitation in the 250–350 nm region a bright emission peaking at 672 nm is observed, whereas a second weaker emission at higher energy (maximum at 576 nm) is detected upon excitation in the 350–500 nm range. Luminescence spectra and corresponding excitation spectra are reported in Fig. 2. The variation of the emission features with regard to the variation of the excitation wavelength is evidenced in Fig. S2 and S3† for powder samples and small crystals of  $[\text{CuI}(\text{piperazine})_{0.5}]_{\infty}$ , respectively. The two emission bands exhibit different lifetimes of *ca.* 4 and 7 μs for the “high energy” (HE) band and the “low energy” (LE) band, respectively (Table 1). Interestingly, at low temperature the LE band is markedly red shifted by 50 nm whilst the HE band is almost unaffected by the temperature (Fig. 2 and Table 1).

Single crystals of  $[\text{CuI}(\text{piperazine})_{0.5}]_{\infty}$  have also been studied by means of laser scanning confocal fluorescence microscopy (LSCM) to confirm the presence of the unusual HE emission in the crystal. The confocal system does not allow

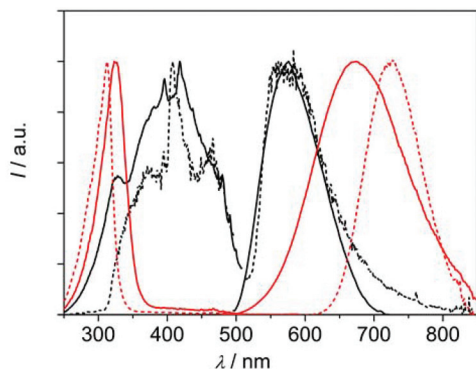


**Fig. 2** Normalized corrected emission (500–850 nm) and excitation (250–500 nm) spectra of solid  $[\text{CuI}(\text{piperazine})_{0.5}]_{\infty}$  at room temperature (solid lines) and at 77 K (dashed lines). Red lines: emission spectra upon excitation at 320 nm and excitation spectra collected on the maxima of the emission spectra at room and low temperature, respectively; black lines: emission spectra upon excitation at 440 nm and excitation spectra collected at 550 nm.

**Table 1** Luminescence properties of  $[\text{CuI}(\text{piperazine})_{0.5}]_{\infty}$  in the solid state

295 K		77 K	
$\lambda_{\text{max}}^a/\text{nm}$	$\tau/\mu\text{s}$	$\lambda_{\text{max}}^a/\text{nm}$	$\tau/\mu\text{s}$
576	4.3 <sup>b</sup>	564	— <sup>d</sup>
672	6.8 <sup>c</sup>	725	22.7 <sup>c</sup>

<sup>a</sup> From corrected emission spectra. <sup>b</sup> Excitation at 465 nm. <sup>c</sup> Excitation at 278 nm. <sup>d</sup> Weak emission.

excitation in the 250–350 nm range while excitation at 405 nm is accessible. Space-resolved fluorescence spectra of the crystals show an emission with maximum at 570 nm (see Fig. 3).

The LE band displays typical features of <sup>3</sup>CC emission, which arises from a mixed iodide-to-copper charge transfer and *d* → *s,p* copper centered excited state:<sup>14,28</sup> large Stokes shift due to the distortion of the CC state with respect to the ground state, lifetime of the order of 10 μs and a pronounced bathochromic shift at low temperature. The nature of the HE band is less straightforward. The occurrence of XLCT transitions can be excluded on the basis of the saturated structure of the piperazine ligand and the spectral invariance with temperature rules out a localized cluster centred origin. Indeed, <sup>3</sup>CC emission usually shifts to the red as the temperature decreases, since the LUMO of the transition is principally copper 4s in character and a reduction of the Cu...Cu distance in the cluster, occurring at low temperature, leads to a stabilization of the CC excited state.<sup>18,19,29</sup> Important information came from theoretical investigations, which assigned the absorption features in the 400–500 nm region to transitions involving HOMO–LUMO orbitals 1-D delocalized along the infinite CuI chain (see discussion below). Though a direct assignment of the HE band to the 1D-delocalized excitation is not straightforward, because of the vibrationally relaxed nature of the emission, we can safely assume a different nature for the HE emission band with respect to the LE band, likely related to the presence of infinite CuI wires in the crystal. The different lifetimes of the two bands support the assumption.

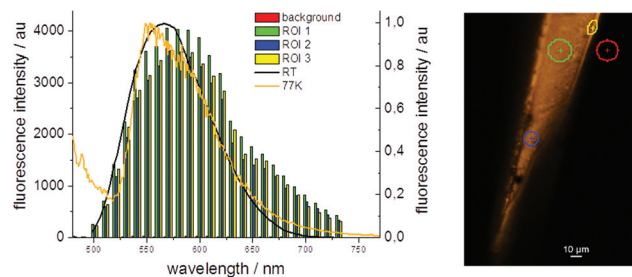


**Fig. 3** Confocal emission spectra of three regions of interest (ROI) compared with the uncorrected emission spectra obtained on the fluorimeter; exc. at 405 nm for the confocal spectra and 440 nm for the fluorimeter spectra. Confocal image of the crystal needle.

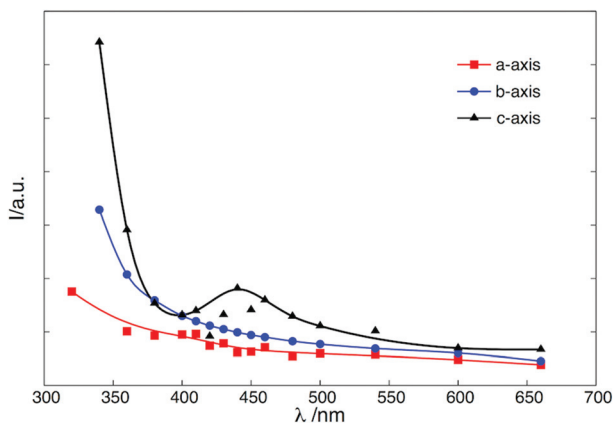


Fig. 4 Directional absorption profiles as simulated through periodic TD-DFT theoretical calculations. The inorganic CuI wire lies along the *c* axis (see Fig. 1).

The dual behaviour of  $[\text{CuI}(\text{piperazine})_{0.5}]_{\infty}$  can thus be rationalized by two emissive non-equilibrated triplet excited states characterized by a localized *vs.* a delocalized nature. This interpretation differs from that given by Xu *et al.*, that tentatively assigned a  ${}^3\text{CC}$  nature to the emission peaking at 567 nm observed upon excitation at 397 nm<sup>24</sup> (the HE band as defined here). In the mentioned case the dependence of the emission features on the excitation wavelength was not explored, and the present study provides a complete characterization of the luminescence properties of  $[\text{CuI}(\text{piperazine})_{0.5}]_{\infty}$  evidencing and discussing its dual behavior.

In order to straighten out the fundamental physics underlying these phenomena, we have investigated the optical absorption properties of the crystalline  $[\text{CuI}(\text{piperazine})_{0.5}]_{\infty}$  by means of theoretical calculations adopting a variant of a Time-Dependent Density Functional Theory (TD-DFT) method<sup>30</sup> recently implemented in the CRYSTAL quantum chemistry *ab initio* code (details in the ESI†).<sup>31</sup> In Fig. 4 we show the simulated excitation profile for the crystal. It is clear that along both *b* and *c* axes the main symmetry-allowed CC excitation (above 300 nm) is present and very intense. Along the *a*-axis the transition is considerably weaker within the range we considered. Along the *c*-axis an additional, less intense excitation is observed in the range 400–500 nm. With reference to Fig. 1, we recall that the *c*-axis is the one along the infinite inorganic CuI wire. The *c*-axis profile in Fig. 4 matches well with the excitation spectra of Fig. 2, where the two separate absorption profiles are evident.

In other words, while the excitation–emission map (Fig. S3†) brings evidence that the two emission bands belong to separate excitations, the *ab initio* calculations (i) confirm the double excitation, thus ruling out the possibility that observed bands are due to impurities and/or instrumental errors, (ii) allow one to observe the directional nature of the second transition, which was not possible experimentally due to the unavailability of large single crystals, and (iii) allow one to characterize the excitation and assign it to a transition

between specific orbitals that belong to the inorganic wire (*vide infra*). The nature of the transition is, in fact, different if we consider the *b* or the *c* direction. Through our TD-DFT method we were also able to characterize these transitions. The strongest component of the excitation is principally located in the Gamma point of the reciprocal space, but the breadth of the bands (specially the conduction ones) leads to a broadening of the excitation bands due to transitions in other points of the Brillouin zone. Along the *b*-axis the transition takes place between the HOMO–1 and LUMO+1 levels. As we report in the ESI,† these are both orbitals belonging to the CuI inorganic part, and are localized. Along the *c*-axis, both bands are to be assigned to a HOMO–LUMO transition. The LUMO, in particular, is very delocalized (see Fig. S4 in the ESI†). Along with the elementary excitation from level to level, there is a particle-hole recombination (exciton) that brings the two levels closer. This leads to a quasi-particle (collective) excitation energy that is lower than the main one and is weaker, but assigned to the same type of excitation.

From these considerations we can conclude that the dual luminescence behavior of  $[\text{CuI}(\text{piperazine})_{0.5}]_{\infty}$  can be ascribed to the presence of both  ${}^3\text{CC}$  transitions, already observed in multinuclear compounds of CuI, and delocalized transitions, peculiar of the 1D infinite inorganic chain. The latter are visible only along one specific direction, and require a high degree of crystallinity of the material. A further evidence of the crystalline character of the LUMO level is represented by the considerable broadness of the LUMO band (see Fig. S4, ESI†). These particular photophysical properties strengthen the idea of exploring copper halide compounds containing inorganic wires in their structure as dual hybrid (inorganic and organometallic) luminescent materials.

## Notes and references

- 1 D. M. Zink, L. Bergmann, D. Ambrosek, M. Wallesch, D. Volz and M. Mydlak, *Transl. Mater. Res.*, 2014, **1**, 015003.
- 2 F. Wei, T. Zhang, X. Liu, X. Li, N. Jiang, Z. Liu, Z. Bian, Y. Zhao, Z. Lu and C. Huang, *Org. Electron.*, 2014, **15**, 3292–3297.
- 3 M. Wallesch, D. Volz, D. M. Zink, U. Schepers, M. Nieger, T. Baumann and S. Bräse, *Chem. – Eur. J.*, 2014, **20**, 6578–6590.
- 4 Z. Liu, J. Qiu, F. Wei, J. Wang, X. Liu, M. G. Helander, S. Rodney, Z. Wang, Z. Bian, Z. Lu, M. E. Thompson and C. Huang, *Chem. Mater.*, 2014, **26**, 2368–2373.
- 5 D. M. Zink, D. Volz, T. Baumann, M. Mydlak, H. Flügge, J. Friedrichs, M. Nieger and S. Bräse, *Chem. Mater.*, 2013, **25**, 4471–4486.
- 6 L. Maini, P. P. Mazzeo, F. Farinella, V. Fattori and D. Braga, *Faraday Discuss.*, 2014, **170**, 93–107.
- 7 D. Volz, D. M. Zink, T. Bockrocker, J. Friedrichs, M. Nieger, T. Baumann, U. Lemmer and S. Bräse, *Chem. Mater.*, 2013, **25**, 3414–3426.

- 8 F. Wei, J. Qiu, X. Liu, J. Wang, H. Wei, Z. Wang, Z. Liu, Z. Bian, Z. Lu, Y. Zhao and C. Huang, *J. Mater. Chem. C*, 2014, **2**, 6333–6341.
- 9 X. Liu, T. Zhang, T. Ni, N. Jiang, Z. Liu, Z. Bian, Z. Lu and C. Huang, *Adv. Funct. Mater.*, 2014, **24**, 5385–5392.
- 10 M. Hashimoto, S. Igawa, M. Yashima, I. Kawata, M. Hoshino and M. Osawa, *J. Am. Chem. Soc.*, 2011, **133**, 10348–10351.
- 11 D. Volz, A. F. Hirschbiel, D. M. Zink, J. Friedrichs, M. Nieger, T. Baumann, S. Brase and C. Barner-Kowollik, *J. Mater. Chem. C*, 2014, **2**, 1457–1462.
- 12 A. Barbieri, G. Accorsi and N. Armaroli, *Chem. Commun.*, 2008, 2185–2193.
- 13 S. Perruchas, C. Tard, X. F. Le Goff, A. Fargues, A. Garcia, S. Kahlal, J.-Y. Saillard, T. Gacoin and J.-P. Boilot, *Inorg. Chem.*, 2011, **50**, 10682–10692.
- 14 P. C. Ford, E. Cariati and J. Bourassa, *Chem. Rev.*, 1999, **99**, 3625–3648.
- 15 N. Armaroli, G. Accorsi, F. Cardinali and A. Listorti, *Top. Curr. Chem.*, 2007, **280**, 69–115.
- 16 S. Perruchas, X. F. Le Goff, S. b. Maron, I. Maurin, F. o. Guillen, A. Garcia, T. Gacoin and J.-P. Boilot, *J. Am. Chem. Soc.*, 2010, **132**, 10967–10969.
- 17 P. P. Mazzeo, L. Maini, A. Petrolati, V. Fattori, K. Shankland and D. Braga, *Dalton Trans.*, 2014, **43**, 9448–9455.
- 18 D. Braga, F. Grepioni, L. Maini, P. P. Mazzeo and B. Ventura, *New J. Chem.*, 2011, **35**, 339–344.
- 19 D. Braga, L. Maini, P. P. Mazzeo and B. Ventura, *Chem. – Eur. J.*, 2010, **16**, 1553–1559.
- 20 F. De Angelis, S. Fantacci, A. Sgamellotti, E. Cariati, R. Ugo and P. C. Ford, *Inorg. Chem.*, 2006, **45**, 10576–10584.
- 21 D. M. Zink, M. Bächle, T. Baumann, M. Nieger, M. Kühn, C. Wang, W. Klopper, U. Monkowius, T. Hofbeck, H. Yersin and S. Bräse, *Inorg. Chem.*, 2013, **52**, 2292–2305.
- 22 M. J. Leitzl, F.-R. Kühle, H. A. Mayer, L. Wesemann and H. Yersin, *J. Phys. Chem. A*, 2013, **117**, 11823–11836.
- 23 R. Czerwieńiec, J. Yu and H. Yersin, *Inorg. Chem.*, 2011, **50**, 8293–8301.
- 24 Q. Hou, J.-H. Yu, J.-N. Xu, Q.-F. Yang and J.-Q. Xu, *Inorg. Chim. Acta*, 2009, **362**, 2802–2806.
- 25 R. Peng, M. Li and D. Li, *Coord. Chem. Rev.*, 2010, **254**, 1–18.
- 26 F. H. Allen, *Acta Crystallogr., Sect. B: Struct. Sci.*, 2002, **B58**, 380–388.
- 27 S. Sculfort and P. Braunstein, *Chem. Soc. Rev.*, 2011, **40**, 2741–2760.
- 28 M. Vitale and P. C. Ford, *Coord. Chem. Rev.*, 2001, **219–221**, 3–16.
- 29 T. H. Kim, Y. W. Shin, J. H. Jung, J. S. Kim and J. Kim, *Angew. Chem., Int. Ed.*, 2008, **47**, 685–688.
- 30 A. M. Ferrari, R. Orlando and M. Rérat, *J. Chem. Theory Comput.*, 2015, DOI: 10.1021/acs.jctc.1025b00199.
- 31 R. Dovesi, R. Orlando, A. Erba, C. M. Zicovich-Wilson, B. Civalleri, S. Casassa, L. Maschio, M. Ferrabone, M. De La Pierre, P. D’Arco, Y. Noël, M. Causà, M. Rérat and B. Kirtman, *Int. J. Quantum Chem.*, 2014, **114**, 1287–1317.